Behavior of Surface-Anchored Poly(acrylic acid) Brushes with Grafting Density Gradients on Solid Substrates: 1. Experiment

Tao Wu,[†,‡] Peng Gong,[§] Igal Szleifer,[§,⊥] Petr Vlček,[∥] Vladimír Šubr,[∥] and Jan Genzer*[,‡]

Department of Chemical & Biomolecular Engineering, North Carolina State University, Raleigh, North Carolina 27695-7905, Department of Chemistry, Purdue University, West Lafayette, Indiana 47907-1393, and Institute of Macromolecular Chemistry, Prague, Czech Republic

Received May 4, 2007; Revised Manuscript Received July 1, 2007

ABSTRACT: We describe experiments pertaining to the formation of surface-anchored poly(acrylic acid) (PAA) brushes with a gradual variation of the PAA grafting densities on flat surfaces and provide detailed analysis of their properties. The PAA brush gradients are generated by first covering the substrate with a molecular gradient of the polymerization initiator, followed by the "grafting from" polymerization of *tert*-butyl acrylate (tBA) from these substrate-bound initiator centers, and finally converting the PtBA into PAA. We use spectroscopic ellipsometry to measure the wet thickness of the grafted PAA chains in aqueous solutions at three different pH values (4, 5.8, and 10) and a series of ionic strengths (IS). Our measurements reveal that at low grafting densities, σ, the wet thickness of the PAA brush (H) remains relatively constant, the polymers are in the mushroom regime. Beyond a certain value of σ, the macromolecules enter the brush regime, where H increases with increasing σ. For a given σ, H exhibits a nonmonotonic behavior as a function of the IS. At large IS, the H is small because the charges along PAA are completely screened by the excess of the external salt. As IS decreases, the PAA enters the so-called salt brush (SB) regime, where H increases. At a certain value of IS, H reaches a maximum and then decreases again. The latter is a typical brush behavior in so-called osmotic brush (OB) regime. We provide detailed discussion of the behavior of the grafted PAA chains in the SB and OB regimes.

Introduction

Surface-anchored polyelectrolyte polymers have at least one of their ends attached to a surface or interface and carry at least one ionizable group on their backbone.[1] Compared to the behavior of neutral polymer brushes, which is rather well understood,[2−4] polyelectrolyte brushes have been investigated to a lesser extent due to their complexity. Depending on the nature of the electrostatic charges along the polymer backbone, one can distinguish between two types of polyelectrolytes: strong and weak. Strong ("quenched") polyelectrolytes have a fixed degree of dissociation, f; their properties thus do not depend on the pH of the solution. In contrast, in weak ("annealed") polyelectrolytes, f depends on pH.

Various theoretical approaches have been utilized to describe the performance of charged macromolecules at interfaces.[5−13] Experimental techniques, which had been used successful to study neutral polymer brushes, are also applied to polyelectrolyte brushes. Among strong polyeletrolytes, polystyrenesulfonate sodium salt PSSNa[14],[15−17] poly(4-vinyl-*N*-*n*-butylpyridinium) bromide BuPVP[18−20] brushes have been studied most extensively. Several groups also performed experiments to investigate the behavior of weak polyelectrolytes anchored at surfaces. For example, Kurihara and Kunitake measured the surface forces between monolayers of anchored poly(acrylic acid) (PAA).[21] They observed that the repulsive forces between two grafted polymeric monolayers increased with increasing salt concentration. Kim et al. prepared a PAA gradient on corona discharge treated polyethylene sheet surface and studied the effects of surface density and counterion size upon the dissociation behavior of grafted PAA.[22] PAA brushes immobilized with a second polystyrene block were also measured at three low pH solutions as a function of the solution ionic strength.[23,24]

The chief theme of our work is to carry out a systematic study of the interfacial properties of surface-grafted PAA as a function of its ionic strength (IS), solution pH, polymer grafting density (σ), and molecular weight (M). In order to systematically study the effect of σ on the interfacial properties of surface-anchored PAA, we utilize a recently developed grafting method,[25,26] which facilitates the formation of assemblies comprising anchored PAA with a gradual variation of grafting densities on one single solid substrate. Because of its simplicity, robustness, and the ability to synthesize polymer brushes with narrow molecular weight distributions, atom transfer radical polymerization (ATRP) will be used to perform the surface-initiated polymerization.[27] Previous studies have revealed that acrylic-based polymers are difficult to polymerize by ATRP because of the interaction of the carboxylic acid functionalities with the ATRP catalyst.[28] Hence, in order to form a surface-anchored PAA with a grafting density gradient, we first synthesize a gradient of poly(*tert*-butyl acrylate) (PtBA) and then converted the PtBA into PAA by hydrolysis.[29−31]

PAA represents an interesting case of charged polymers. Its relatively simple structure enables the investigation of the charge effect on the properties of surface-anchored polymers; understanding of such model systems can provide important guidance for comprehending the characteristics of more complex charged assemblies, including biopolymers. In the past, PAA brushes have been utilized in a large variety of studies involving: control liquid and solute transport (separation) through (in) membranes,[32] study microstructures of multiblock copolymers,[33] study interactions in charged systems,[34] study protein[35] and

* Corresponding author. E-mail: Jan_Genzer@ncsu.edu. Telephone: +1-919-515-2069.
† Present address: Intel Corporation, Chandler, Arizona 85226-3699.
‡ Department of Chemical & Biomolecular Engineering, North Carolina State University.
§ Department of Chemistry, Purdue University.
∥ Institute of Macromolecular Chemistry.
⊥ Present address: Department of Biomedical Engineering, Northwestern University, Evanston, IL 60208-3100.

10.1021/ma0710176 CCC: $37.00
Published on Web 10/26/2007

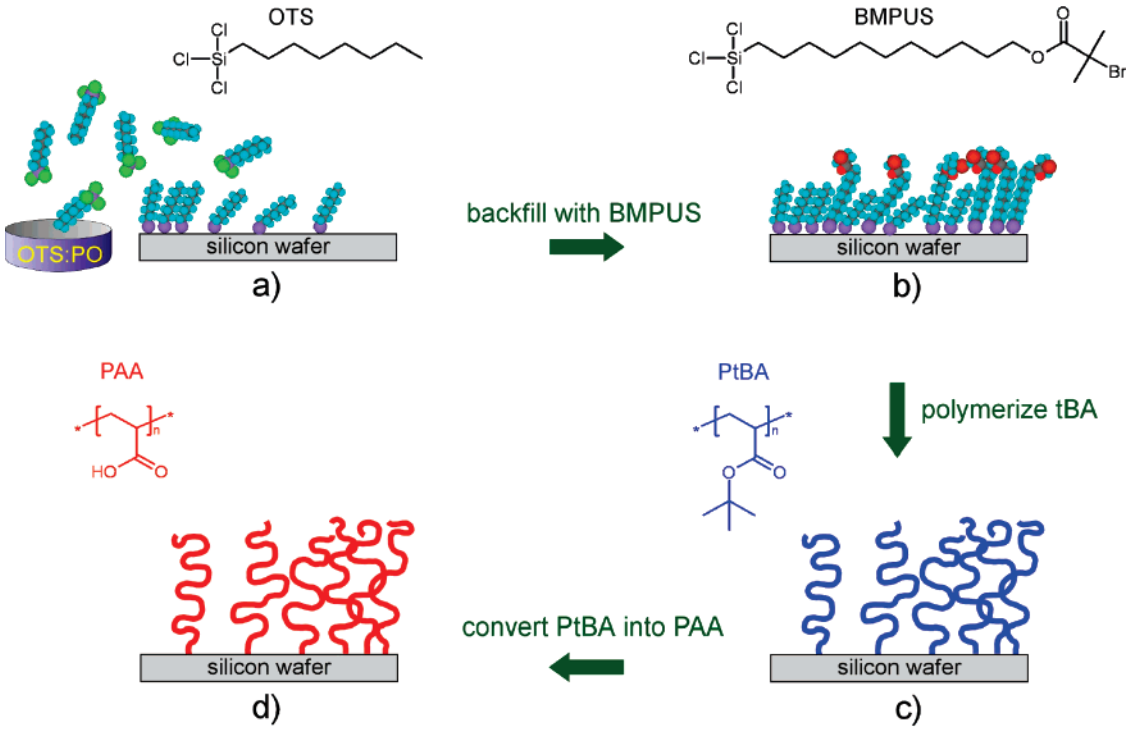

Figure 1. Schematic illustrating the formation of poly(acrylic acid) (PAA) assemblies grafted on flat surfaces having gradient rafting density. (a) A molecular gradient of *n*-octyl trichlorosilane, (OTS) is formed on the surface by vapor deposition technique. The flux of the OTS molecules in the vapor phase is regulated by adjusting the composition of OTS and paraffin oil (PO) in the diffusion source. As OTS evaporates, it diffuses in the vapor phase and generates a concentration gradient along the silica substrate. Upon impinging on the substrate, the OTS molecules react with the substrate-bound −OH functionalities and form an OTS self-assembled monolayer (SAM). (b) The regions on the surface not covered with OTS are backfilled with 1-trichlorosilyl-2-(*m*−*p*-chloromethylphenyl)ethane (CMPE), ATRP initiator. (c) Surface-grafted assemblies of poly(*tert*-butyl acrylate) are formed on the substrates by "grafting from" ATRP of tBA as described in the text. d) the PtBA is converted into PAA by chemically cleaving off the *tert*-butyl group, following the procedure outlined in the text.

enzyme[36] adsorption/immobilization, perform attachment of ionic surfactants,[37] create "smart"/responsive surfaces,[38] fabricate templates for formation and ordering of nanoinclusions,[39] and also test theories of polyelectrolytes brushes,[40] We have previously reported preliminary results in a separate monograph.[41]

In this paper, we expand upon our previous work and describe the formation of PAA assemblies with gradual variation of chain grafting densities on the substrate and present experimental results revealing the dependence of the PAA layer thickness as a function of σ, IS, and pH. We also compare the experimentally observed trends in H to the predictions of existing scaling models. In the following paper,[42] we discuss the effect of the PAA molecular weight on PAA brush behavior. We also use molecular theory of charged polymer brushes to reproduce selected experimental findings and provide molecular insight into parameters that are either hard to measure or are not experimentally accessible.[42]

Experimental Section

Materials. ω-Undecylenyl alcohol, 2-bromoisobutyryl bromide, pyridine, platinum(0)-1,3-divinyl-1,1,3,3-tetramethyldisiloxane complex solution (2% in xylene solution), *tert*-butyl acrylate, copper(I) bromide (CuBr), *N*,*N*,*N*′,*N*′-pentamethyldiethyenetriamine (PMDETA), were obtained from Aldrich. *N*-Octyltrichlorosilane (OTS) was obtained from Gelest. All solvents used were obtained from Aldrich. Unless specified otherwise, all the chemicals were used as received.

Initiator Synthesis. The ATRP initiator used in this study was (11-(2-bromo-2-methyl)propionyloxy)undecyltrichlorosilane, Br-$(CH_3)_2CCOO(CH_2)_{11}SiCl_3$ (BMPUS); it was synthesized following a two-step procedure developed by others.[43] During the second step, we used 10 μL of platinum(0)-1,3-divinyl-1,1,3,3-tetramethyldisiloxane complex solution as the catalyst instead of the Karstedt catalyst. Toluene and tetrahydrofuran were dried with sodium sulfate and filtered before use. The structure of the synthesized initiator was confirmed by NMR experiments.

Surface Polymer Gradient Formation. Following the procedure illustrated in Figure 1, a gradient of *n*-octyltrichlorosilane (OTS) monolayer was first formed by the vapor diffusion technique,[44] where the OTS:paraffin oil ratio was kept 1:2 and the diffusion time was 2 min. The regions on the substrate unmasked by the OTS molecules were then backfilled with the BMPUS initiator by placing the OTS gradient-covered silicon wafers into a toluene solution of BMPUS (20 μL of BMPUS in 20 mL of anhydrous toluene) for 18 h at −10 °C without stirring.[45] After the initiator deposition, the samples were removed from the solution, thoroughly washed with toluene, acetone, and ethanol, and dried with nitrogen. Ellipsometry measurements confirmed that only a single self-assembled monolayer of both OTS and BMPUS was formed on the silica substrates.

Surface-initiated polymerization of poly(*tert*-butyl acrylate) (PtBA) was performed by atom transfer radial polymerization (ATRP), as described earlier.[41] Copper(I) bromide (CuBr) (0.1564 g, 1.1×10^{-3} mol) and copper(II) bromide ($CuBr_2$) (0.012 g, 4.2×10^{-5} mol) were added to a dry Teflon-capped vial, followed by adding deoxygenated acetone (1.6 g) and *tert*-butyl acrylate (tBA) (14.0 g, 1.08×10^{-1} mol). After the solution was purged with nitrogen for 5 min, 240 μL (1.14×10^{-6} mol) of *N*,*N*,*N*,*N*′,*N*′-pentamethyldiethylenetriamine (PMDETA) was added. The solution was stirred until the Cu complex formed. After the complex formation, the gradient-covered silicon wafers were placed into the solution. The solution was purged with nitrogen for 2 min, and then the vial was sealed and placed in a temperature controlled oil bath set at 60 °C. After a predetermined reaction time, the samples were removed and washed thoroughly with acetone and methanol and dried with nitrogen. The silica substrates covered with a PtBA gradient were then placed into a flask, which contained a mixture

of 20 mL of 1,4-dioxane and 3 mL of concentrated HCl (37%). The flask was connected to a condenser, and the solution was heated to reflux. The samples were removed after 2−5 h (see Discussion below) and thoroughly washed with deionized water and methanol.

Solution Polymerization and Hydrolysis of PtBA. Solution polymerization of tBA under the same reaction condition was also performed, where methyl 2-methyl-2-bromopropionate (240 μL, 2.2 $\times$ 10^{-3} mol) was added as a solution initiator instead of the BMPUS-covered silicon wafer. After the polymerization, the solutions were precipitated into a 15-fold excess of a 50:50 water: MeOH (v/v) bath. After the solvent was decanted off, the polymer was redissolved in diethyl ether; the solution turned deep blue. After catalyst removal, the polymer solution was reprecipitated until the polymer remained white. The final polymer was dried under vacuum. The obtained PtBA was used to estimate the corresponding molecular weight of polymer brush grown from the substrate.

A portion of the PtBA obtained from solution polymerization was converted to PAA by adding PtBA (2.5 g) to a solution of 20 mL of dioxane and 3 mL of concentrated HCl (37%). The solution was heated at the reflux temperature. After a 5 h reaction, the solution was cooled and a part of the excess reagents ($\approx$10 mL) was removed by evaporation under vacuum. Subsequently, the PAA solution was precipitated into 200 mL of methyl ethyl ketone (MEK). After the solvent was decanted off, the polymers were dried under high vacuum overnight.

SEC Measurement. The PtBA SEC experiments were conducted at 20 °C using a HLPC instrument (Labora, Czech Republic) equipped with a two-column separation system (Polymer Standards Service GmbH, Germany, porosities 10^5 and 10^3 angstroms) in tetrahydrofuran as the mobile phase. The flow rate was 1 mL/min and the concentration of samples for injection was approximately 1% (w/w). The system was calibrated with PMMA standards (Polymer Standards Service GmbH, Germany). Eluograms were analyzed using a software Caliber (Polymer Laboratories, USA) and the Mark−Houwink−Sakurada equation, $[\eta] = KM^a$, where $[\eta]$ is the intrinsic viscosity, with $K = 3.3 \times 10^{-5}$ and $a = 0.80$.[46] The system is equipped with two detectors: differential refractometer RIDK-102 (Laboratorní Prístroje, Czech Republic) and UV detector LCD-2040 (ECOM, Czech Republic) with adjustable wavelength. The polymer weights were calculated from the RI traces. After the conversion of PtBA to PAA, the molecular weight of PAA was also determined by SEC by using Superose 12 column (Äkta Explorer, Amersham Bioscience) equipped with differential refractometer and multiangle light scattering detector DAWN DSP-F (Wyatt Technology Corp.). A 0.3 M sodium acetate buffer (pH $\approx$ 6.5) was used as the mobile phase. The flow rate was 0.5 mL/min.

The molecular weight of PtBA synthesized in solution for 10 h was $M_n = 8.56$ kDa with $M_w/M_n = 1.15$. The molecular weight of PAA was $M_n = 4.10$ kDa with $M_w/M_n = 1.29$. The numbers of repeat units were about 67 and 57 for PtBA and PAA, respectively. The molecular weight of PAA calculated from the PtBA SEC measurements (4.81 kDa) is in a reasonable agreement with the direct PAA measurements (the accuracy of $\pm$ 15%). In the data analysis that follows, we are going to use the degree of polymerization of PAA that was calculated from the PtBA SEC measurements. We justify our choice by the fact that, in contrast to PAA, PtBA is a neutral polymer, which is insensitive to the pH and ionic strength of the mobile phase. We thus believe that the PtBA SEC measurements are more accurate.

Ellipsometry Measurements and Determining Grafting Density. The thickness of the SAM and the polymer film was measured using a single-wavelength fixed geometry ellipsometer (AutoEL II, Rudolph Technologies) and a variable angle spectroscopic ellipsometry (J.A. Woollam, Inc.). The thickness was evaluated from the experimentally measured ellipsometric angles Ψ and Δ using the supplied software (DafIMB and WVASE32). The following refractive indices were used for various material: 1.45 for SAMs,[47] 1.466 for poly(*tert*-butyl acrylate),[48] and 1.527 for poly(acrylic acid).[47] The grafting density (σ) of the surface-anchored PAA brushes was calculated from the dry polymer thickness (h) using $\sigma = h\rho N_A/M_n$, where ρ is the density of PAA (= 1.1 g/cm^3),[47] N_A is the Avogadro's number, and M_n is the polymer molecular weight. While h can be accessed directly on the gradient sample, values of M_n at different positions on the specimens are not available. As in our previous work, we thus used M_n values for polymers grown in the bulk, like others,[18−20] and assume that, to the first approximation, all chains had the same degree of polymerization along the substrate (i.e., the polymerization rate was independent of the grafting density of the initiator on the substrate; see refs 25 and 26 and a note[49]). We stress that the molecular weight of the solution-grown polymers only resembles that of the polymers prepared on the flat substrate because of different sterical constrains imposed on the polymers grown in these two different geometries. Nevertheless, this is best approximation we can make at this point; we have already used it successfully in our previous work.[25,26]

Table 1. Example of Adjusting the Ionic Strength of a pH = 4 Solution

75 mL cell solution ionic strength	amount of aqueous solution (mL) replaced by the NaCl solution (concn = 2 M, pH = 4)
1.0×10^{-4}	
1.0×10^{-3}	0.034
5.0×10^{-3}	0.150
1.0×10^{-2}	0.188
1.0×10^{-1}	3.392
5.0×10^{-1}	15.789
7.5×10^{-2}	12.500
1.0×10^{0}	15.000

The wet thickness of the PAA in aqueous solutions was measured by placing the samples in a custom-designed solution cell, incubating them for a desired period of time (typically >5 h) and performing the experiments with VASE at $\phi = 70°$, where ϕ is the angle between the incoming beam and the sample normal. The ellipsometric angles Ψ and Δ were collected for a series of wavelengths ranging from 240 to 1000 nm. The wet PAA thickness was evaluated using a graded effective medium approximation model based on linear combination of the optical constants of the DI water and PAA.

The pH and the ionic strength of the aqueous solution in the cell were adjusted as follows. A desired amount of aqueous solution was removed and a replaced with the corresponding amount of concentrated NaCl, HCl, or NaOH solutions. In the following we illustrate the procedure used to prepare a solution with the pH = 4 and various ionic strengths. First, the ellipsometric cell was filled with 75 mL of aqueous solution, followed by adding 75 μL of 0.1 M HCl in order to obtain solution with pH = 4. We also prepared a stock NaCl solution (concentration = 2 M and pH = 4). The right column in Table 1 lists the corresponding amounts of the aqueous solution that was replaced with the NaCl in order to prepare the ionic strength listed in the left column of Table 1.

NEXAFS Measurements. Near-edge X-ray absorption fine structure (NEXAFS) spectroscopy was used to study the spatial concentration of PAA on the sample substrates.[50] The NEXAFS experiments were carried out on the U7A NIST/Dow Materials Soft X-ray Materials Characterization Facility at the National Synchrotron Light Source at Brookhaven National Laboratory (NSLS BNL). The NEXAFS spectra were collected in the partial electron yield (PEY) at the so-called "magic" angle ($\theta = 55°$) incidence geometries, where θ is the angle between the sample normal and the polarization vector of the X-ray beam.

FTIR Spectroscopy Measurements. Fourier transform infrared (FTIR) spectroscopy was collected in the transmission mode with Nicolet 750. A total of 1024 scans were collected with resolution 8 cm^{-1} for each measurement. A bare silicon wafer was used as the blank. The IR spectra for polymer bulk were measured with the KBr pellets. The IR spectra were analyzed using the OMNIC 5.0 software.

Experimental Results

FTIR measurements were performed to characterize the bulk and surface-grafted polymers before and after the hydrolysis of

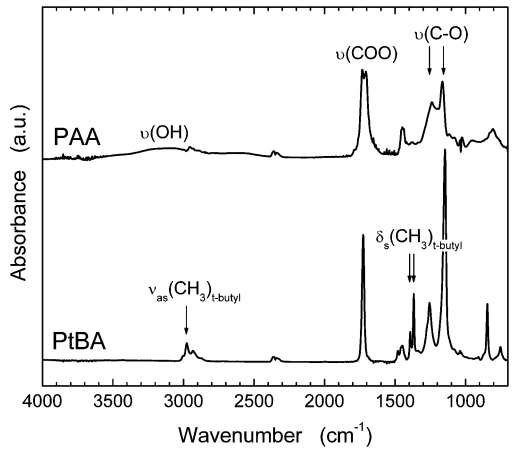

Figure 2. FTIR spectra from the KBr pellets containing PtBA (bottom) and PAA (top) prepared using the bulk solution polymerization.

the PtBA. The FTIR spectra of PtBA and PAA from solution polymerization are depicted in the bottom and top of Figure 2, respectively. The characteristic peaks of the *tert*-butyl group, which exist only in PtBA, are detected at 2979 cm^{-1} ($\nu_{as}(CH_3)$) and 1393/1368 cm^{-1}($\delta_s(CH_3)$). The disappearance of those peaks in the PAA IR spectra confirms the completion of the hydrolysis of PtBA. The broad band at 3200 cm^{-1} in the PAA IR spectra is attributed to the −OH group formed during the PtBA conversion.

The spectra for PtBA and PAA brush on substrates (see Supporting Information) exhibit very similar trends reported for the bulk PtBA and PAA specimens (cf. Figure 2). As expected, the absolute IR intensities from the latter set of samples are weaker due to the smaller number of polymer chains analyzed. The disappearance of the peaks corresponding to $\nu_{as}(CH_3)$ (at 2979 cm^{-1}) and $\delta_s(CH_3)$ (at 1393 and 1368 cm^{-1}) in the PAA/Si spectra, relative to the PtBA/Si samples, provides evidence that the hydrolysis of poly(*tert*-butyl acrylate) took place.

FTIR spectra were taken at various positions along the PtBA-covered specimen to verify that a gradient in grafting density of the PtBA was formed on the substrate. In order to generate noticeable change of peak intensity along the gradient, the gradient with rather long polymerization time (24 h) was prepared. In Figure 3, we plot FTIR spectra collected along the PtBA gradient. The increase in the intensities of the two characteristic peaks of PtBA corresponding to ν(COO) (at 1733 cm^{-1}) and $\nu_{as}(CH_3)_{tert-butyl}$ (at 2979 cm^{-1}) is indicative of the gradually increasing concentration of PtBA on the substrate as one traverses across the specimen from the OTS-rich side (low values on the "Position on substrate" coordinate) toward the BMPUS-rich side. The experimental results confirm that the polymer brush thickness or density varies along the gradient.

While FTIR proved useful in confirming that the conversion of PtBA into PAA took place, it did not provide sufficient information about the thickness of the polymers on the substrate. Spectroscopic ellipsometry was used to measure the dry thickness of both the PtBA and PAA gradient samples, which were polymerized for 10 h and hydrolysis in HCl/dioxane bath for 10 h. In Figure 4, we plot the dry thickness of PtBA (solid symbols) and PAA (open symbols) as a function of the position on the substrate. The data in Figure 4 reveal that the thickness of both PtBA and PAA increases as one moves from the OTS side (small number on the abscissa) of the sample toward the initiator-covered side (large numbers on the abscissa); in both cases, the functional form closely resembles that of a backward diffusionlike profile.

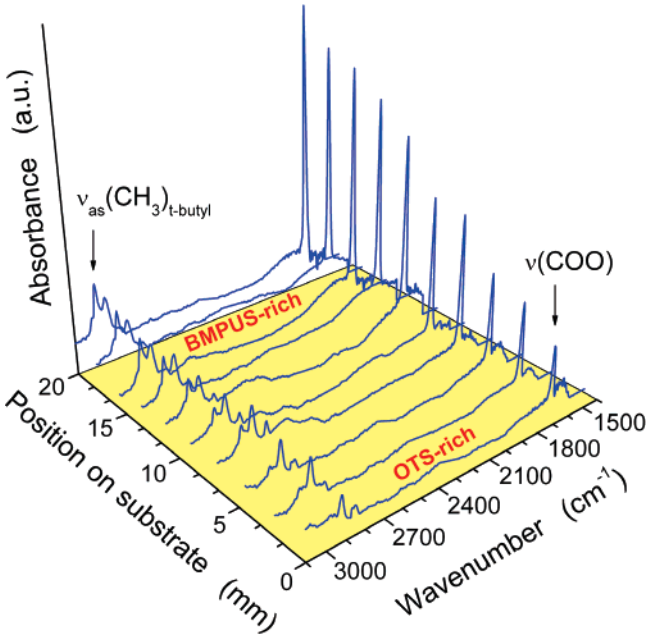

Figure 3. FTIR spectra of PtBA grafting density gradient as a function of the position on the substrate. The PtBA was polymerized for 24 h from the substrate covered with the gradient of the ATRP initiator.

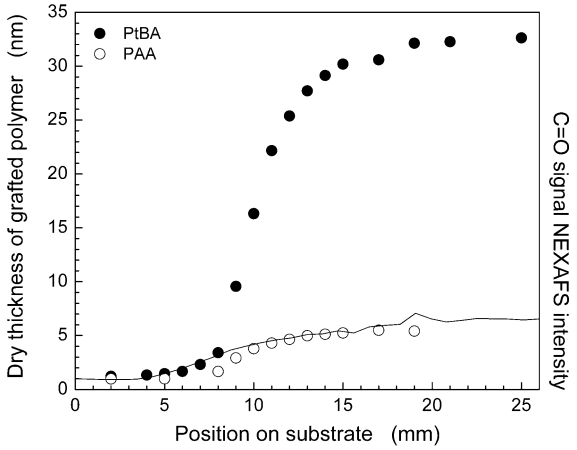

Figure 4. Dry thickness of PtBA (solid symbols) and PAA (open symbols) as a function of the position on the substrate. The solid line represents the PEY NEXAFS intensity measured at $E = 531$ eV on the PAA sample as a function of the position on the substrate.

Assuming that all chains of both PtBA and PAA have the same degree of polymerization along the substrate, the increase of the polymer dry thickness can be attributed to the increase of the polymer grafting density on the substrate. There is a rapid decrease in the dry polymer thickness after the hydrolysis. Specifically, the thickness of PtBA decreases 6-fold upon hydrolysis to PAA. The decrease seems to scale proportionally with the grafting density of PtBA on the substrate. In order to understand this behavior, a series of homogeneous polymer brush were prepared and followed by the PtBA-to-PAA conversion measurements. Specifically, PtBA brushes were first grown on silicon substrates that were covered homogeneously with the surface-bound initiators. The hydrolysis of PtBA on the Si wafer was performed as a function of the reaction time. We will return to this point later in our discussion.

Experiments using NEXAFS were conducted in order to evaluate the density of PAA as a function of the position on the substrate. With the X-ray monochromator set to 531 eV, which corresponds to the 1s → $\pi^*_{C=O}$ transition, we collected the partial electron yield (PEY) NEXAFS signal by scanning

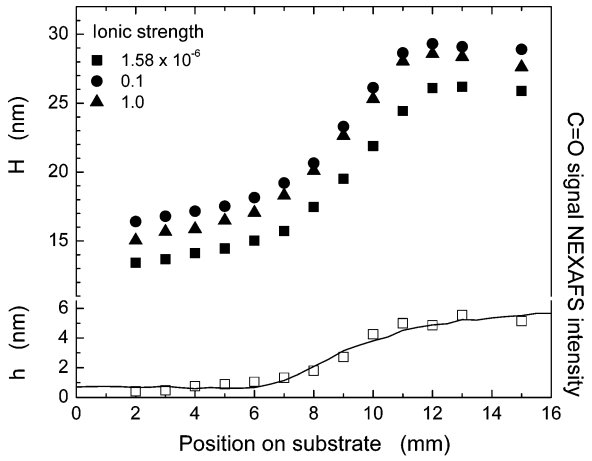

Figure 5. Dry (*h*) and wet (*H*) thickness of PAA measured as a function of the position on the solid substrate. The wet thickness was evaluated at pH = 4 and is plotted as a function of three different ionic strengths. The solid line represents the PEY NEXAFS intensity measured at E = 531 eV on the dry PAA sample.

the X-ray beam along the gradient. The solid line in Figure 4 depicts the variation of the PEY NEXAFS intensity corresponding to the C═O bond across the PAA gradient. The NEXAFS results confirm that the C═O intensity, and thus the amount of PAA on the surface, increases as one moves along the gradient. The NEXAFS data are in good agreement with the ellipsometric thickness data of PAA.

In order to study the solution properties of the surface-grafted PAA, we incubated the PAA gradients under aqueous solutions under the different pH values (4, 5.8, and 10) and a series of ionic strengths for each pH. Hence, by measuring the wet thickness (*H*) of PAA along the gradient at different solution condition, we obtained the wet thickness profile of the grafted polymer layer as a function of the PAA grafting density, pH, and ionic strength. In Figure 5 we plot an example of a series of measurements performed with one 10 h polymerization sample. The open symbols represent the dry PAA thickness measured as a function of the position on the substrate. The solid line is the PEY NEXAFS intensity scan at E = 531 eV, corresponding to the C═O peak. In the same figure we also plot *H* of PAA measured at pH = 4 and three different ionic strengths. The data show that for all ionic strengths, *H* increases with increasing grafting density of PAA on the substrate. A close inspection of the data in Figure 5 reveals that *H* is a nonmonotonic function of the ionic strength. Specifically, as the ionic strength increases, *H* also increases, reaches a maximum, and then decreases. We will address this behavior in the Discussion section that follows.

Discussion

Surface Hydrolysis of PtBA. We monitored the kinetics of the conversion of PtBA into PAA by measuring the time dependence of the PtBA thickness and contact angle on conversion time on homogeneous PtBA brushes, which were prepared on flat silica substrates covered with a homogeneous distribution of the surface-bound initiator. Figure 6 summarizes the results of our experiments performed on several samples with different initial PtBA dry thicknesses. In Figure 6a, we plot the dry thickness of PtBA, h, normalized by initial film thickness, $h(t = 0)$, as a function of the conversion time. The data show that, for all samples studied, the initial thickness decreases rapidly by about 50% within the first 80 min, followed by a slower decrease at later times.

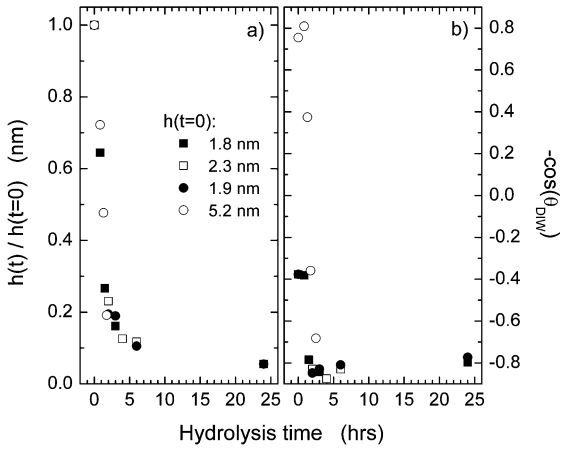

Figure 6. Dry thickness (a) and contact angle (b) of a PtBA/PAA sample as a function of the hydrolysis time. The various symbols denote samples with a different initial dry thickness.

Table 2. Molecular Parameters of PtBA and PAA

	PtBA	PAA
M_o (g/mol)	128.17	72.065
ρ (g/cm^3)	1.05[a]	1.22[b]
v_o (cm^3)	2.027×10^{-22}	9.81×10^{-23}

[a] It is the value for poly(*sec*-butyl acrylate) from: *Polymer Handbook*; Brandrup, J., Immergut, E. H., Grulke, E. A., Eds; Wiley & Sons: New York, 1999. [b] Brandrup, J., Immergut, E. H., Grulke, E. A., Eds.; *Polymer Handbook*; Wiley: New York, 1999.

We attribute the sharp drop in the film thickness to the decrease of the volume of the polymer, associated with the removal of the bulky *tert*-butyl groups. We note that similar behavior has been observed by others.[43] We attribute that the slower decease in PtBA thickness to possible cleavage of the polymer from the substrate, which is caused by the hydrolysis of the ester group inside the initiator (a primary ester). However, since the reaction rate for *tert*-ester hydrolysis is much faster than that for primary-ester hydrolysis, we can complete the conversion of PtBA to PAA before the polymers are completely cleaved off from the substrate.

We make a simple estimate in order to verify our hypothesis. In Table 2, we list the molecular parameters of PtBA and PAA, such as the monomer molecular weight (M_o), the density (ρ), and the volume of the monomer unit (v_o). The latter was calculated by using eq 1:

$$v_o = \frac{M_o}{\rho N_A} \tag{1}$$

where N_A is Avogadro's number.

Assuming that the degree of polymerization of PtBA is the same as that of PAA and the total number of polymer chains upon hydrolysis remains constant, we can use the values in Table 2 to estimate the change in thickness of the PtBA film associated with complete conversion of the PtBA into PAA as

$$\frac{\Delta h_{PtBA}}{h_{init,PtBA}} = \frac{\Delta v_o}{v_{o,PtBA}} = 1 - \frac{v_{o,PAA}}{v_{o,PtBA}} \approx 0.52 \tag{2}$$

where Δh_{PtBA} and $h_{init,PtBA}$ are the PtBA thickness change upon hydrolysis and the initial PtBA thickness, respectively.

This simple estimate illustrates that complete hydrolysis of PtBA into PAA will result in about 52% decreases of the total PtBA film thickness. It also confirms our earlier hypothesis, namely that the rapid drop in polymer thickness within the first

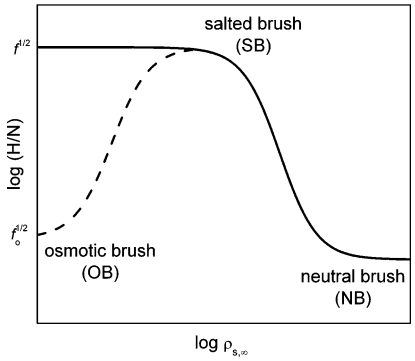

Figure 7. Dependence of the brush thickness reduced by the number of polymer repeat units for monovalent co-ions, *H*/*N*, on the concentration of the external salt, φ_s, for strong (solid line) and weak (dashed line) polyelectrolyte brushes in neutral brush (NB), salted brush (SB), and osmotic brush (OB) regimes. *f* and f_o denote the bulk and "internal" (for weak polyelectrolyte brushes only) degree of dissociation, respectively.

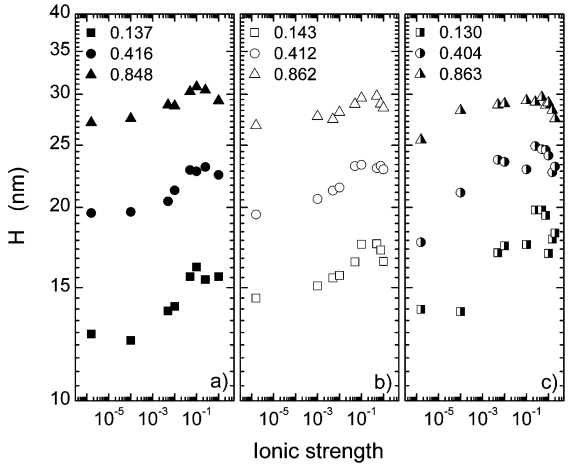

Figure 8. Wet thickness of PAA (*H*) as a function of the solution ionic strength at (a) pH = 4, (b) pH = 5.8, and (c) pH = 10. The symbols represent different grafting densities of PAA in chains/nm^2.

2 h of HCl treatment is associated predominantly with the PtBA to PAA conversion. On the basis of this estimate, HCl treatment times longer than about 2 h would result in some cleavage of the polymer from the substrate. For example, based on the data in Figure 6, after 5 h of hydrolysis, the original thickness of PtBA decreases by 85%.

In Figure 6b, we plot the negative cosine of the DI water contact angle, θ_{DIW}, as a function of the PtBA-to-PAA conversion time. Note that the trend is similar to the PtBA thickness *versus* time behavior. Specifically, θ_{DIW} drops down from 88° (a thick PtBA layer) rather rapidly within the first about 2−3 h, a behavior that is associated with the conversion of the *tert*-butyl group into the −OH group. The contact angle reaches a minimum at about 5 h, after which time is starts to increase slightly again. The latter trend is attributed to the surface exposure of the undecyl silane groups that remain grafted to the substrate after the cleavage of the *tert*-ester in the initiator molecule. In our gradient samples, we performed the PtBA hydrolysis for 5 h in order to ensure the complete removal of *tert*-butyl groups. Although some polymer may have been cleaved off the surface during this extended hydrolysis, a large enough amount of polymer remained on the surface that was used in further analysis. In fact, NEXAFS experiments on PAA samples prepared by hydrolyzing a PtBA sample for about 10 h revealed that a significant amount of PAA still remained on the surface.

Dependence of H on Ionic Strength. Before we discuss our experimental findings pertaining to the polymer thickness dependence on solution ionic strength, we start by briefly describing some theoretical predicted behavior of polyelectrolytes immersed in solutions of monovalent salt ions. A more elaborate treatment of weak electrolyte brushes is presented in the following paper.[42] For a strong (quenched) polyeletrolyte, at high salt concentration (φ_s) the φ_s inside and outside the brush is about the same and the electrostatic interactions are largely screened. Under such conditions, the polyelectrolyte brush behaves exactly as a neutral brush (NB). When the external salt concentration decreases, there is an unbalance in the ion concentration inside and outside the brush because the polymer charge density inside the brush ($f\varphi$, where φ is the polymer volume fraction) is no longer negligible with respect to φ_s. The system enters the salted brush (SB) regime. Because of the electrostatic interactions inside the brush, a salted brush is more extended than a neutral one. As shown schematically in Figure 7, the brush expansion increases with decreasing φ_s. If the external salt concentration is further decreased such that $\varphi_s << f\varphi$, the co-ions are effectively expelled from the brush. In this so-called osmotic brush (OB) regime, the limiting brush thickness is reached, which is independent of φ_s.

The behavior of weak polyelectrolyte brushes is different from that of strong polyelectrolytes in that the number of the backbone charges is not fixed. When there is an excess of salt, as in the NB and SB regimes, [H^+] inside and outside the brush is approximately equal, and the internal degree of dissociation is the same as that in the bulk solution. When the system enters the OB regime, a significant electric potential difference develops between the brush and the bulk solution. In addition, [H^+] inside the brush is considerably higher. As a consequence, the weak charge groups respond to the unfavorable electrostatic condition in OB by discharging themselves. Such a response is impossible for strong brushes, which have a fixed *f*. Figure 7 illustrates the different behavior of weak polyelectrolyte brushes in the OB regime. Because of the discharging process ($f_o < f$), a weak brush in the OB regime is less expanded than the strong brush. As a result, *H*/*N* passes through a maximum as a function of φ_s, being small for both high and small φ_s. Israëls et al. suggested[10] that the salt concentration (φ_s^{max}) corresponding to the maximum of *H*/*N*, which is also the value of φ_S at the transition between the OB and SB regimes, is related to the bulk degree of dissociation and polymer grafting density:

$$\varphi_s^{max} \sim \sigma(f)^{1/2} \tag{3}$$

In Figure 8, we plot the dependence of the PAA wet thickness (*H*) on the solution ionic strength (IS) at pH equal to (a) 4, (b) 5.8, and (c) 10 for three different grafting densities, approximately equal for all three samples. Since only NaCl, HCl, and NaOH were used to change the solution ionic strength, the salt concentration (φ_s) in this case is equal to the solution ionic strength (IS). The data in Figure 8 reveal that *H* depends on IS in a nonmonotonic fashion. Specifically, as IS increases, *H* increases before reaching a maximum at a certain value and then starts to decrease. This behavior, observed for all pH values at all grafting densities (σ), is in accord with the theoretically predicted trends[10] that divide the *H* vs IS dependence into the osmotic brush (OB) and the salted brush (SB) regimes (cf. Figure 7).

The results are also in a very good agreement with the theoretical predictions.[10] Clearly, the ionic strength, at which the transition between the OB and SB regimes occurs (IS_{max}),

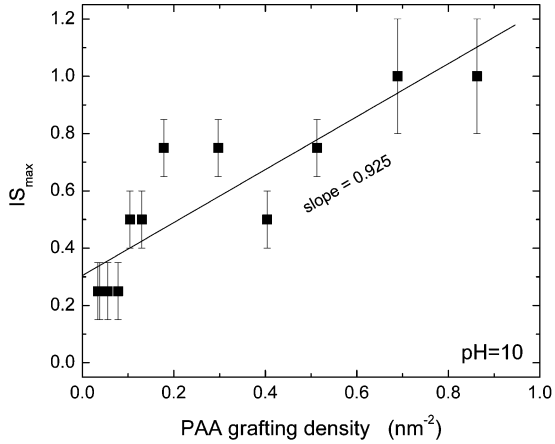

Figure 9. Values of the ionic strength at the boundary between the osmotic brush (OB) and salted brush (SB) regimes (IS_{max}) as a function of grafting density of PAA at pH = 10. The line represents the least-squares fit to the data with the slope given in the text. The error bars represent the uncertainties associated with estimating the values on the ordinate (estimated from the data in Figure 8).

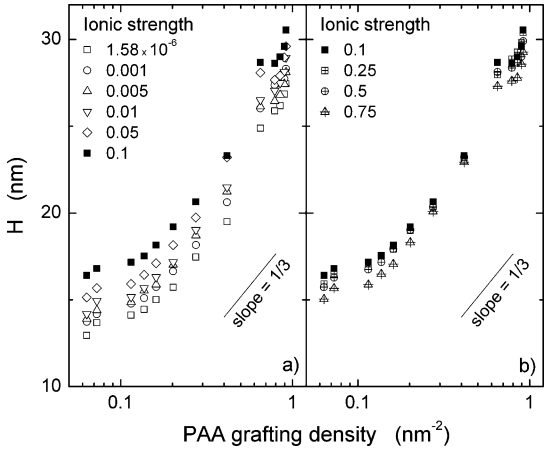

Figure 10. Wet thickness at pH = 5.8 for poly(acrylic acid) (M_n = 4.8 kDa) as a function of the grafting density and ionic strength of the aqueous solution in the (a) osmotic brush (OB) regime and (b) the salted brush (SB) regime. The symbols represent different ionic strength values.

is related to σ and pH, which directly influence f. At pH = 4, IS_{max} is nearly constant regardless of the grafting density σ (Figure 8a), where the degree of dissociation is rather small. At pH = 5.8, f is about 0.5,[24] which explains the relative small shift in IS_{max} (Figure 8b). At pH = 10, IS_{max} shifts significantly (Figure 8c). In Figure 9, we plot the IS_{max} values as a function of σ from all the measurements done at pH = 10. The slope (=0.925) is close to the expected value of 1, since f is close to 1 at pH = 10 (complete ionization), so $IS_{max} \sim \sigma$.

Dependence of H on Grafting Density. In order to study the effect of grafting density on weak polyelectrolyte brush wet thickness in a "conventional" manner, one would have to prepare a large number of polymer brush specimens, each bearing a different grafting density. This rather cumbersome approach precludes establishing systematically the relationship between the PAA brush height and the PAA grafting density.[6,7] Our methodology removes this limitation by proving a simple method for preparing surface-grafted PAA assemblies with variable grafting densities on a single sample.

As mentioned above, the behavior of weak polyelectrolyte brush is complicated, since the dissociation constant f along the polymer backbone depends on the proton concentration in the surrounding polymer solution, $[H^+] = 10^{-pH}$, and is given by $f/(1 - f) = K/[H^+]$, where K is the monomer dissociation constant. When there is an excess of salt in bulk solution, as in the NB and SB regimes (cf. Figure 7), $[H^+]$ values inside and outside the weak polyelectrolyte brush are approximately equal, and the internal degree of dissociation is the same as that in the bulk solution. Hence, the theoretical modeling predicts the scaling relation for H/N in the NB and SB regimes is[6]

$$H \sim N\sigma^{1/3}\left(\frac{f^2}{\varphi_S}\right)^{1/3} \tag{4}$$

When the system enters the OB regime with low salt concentration, a significant electric potential difference develops between the brush and the bulk solution. In addition, $[H^+]$ inside the brush is considerably higher. As a consequence, a portion of the brush charges associate with protons and $f_o/(1 - f_o) = K/(\sigma f_o^{1/2})$, where f_o is the "internal" degree of dissociation. This value of f_o may be much smaller than the value in the bulk (f); the weak groups respond to the unfavorable electrostatic condition in OB by discharging themselves. The brush height in the OB regime is predicted to scale as[6]

$$H \sim N\sigma^{-1/3}\left(\frac{f}{1-f}\right)^{1/3}([H^+] + \varphi_S)^{1/3} \tag{5}$$

Because of the discharging process ($f_o < f$), a weak brush in the OB regime is less expanded than the strong brush. As a result, H/N passes through a maximum as a function of φ_s, being small for both high and small φ_s. The unusual feature that at low φ_s the brush contracts with decreasing φ_s is a typical property of weak groups, which can respond to a change in the local environment. By equating the expressions for H given in eq 4 and 5, the value of φ_S at the transition between the OB and SB regimes scales as eq 3.[10]

Since theories predicted that the scaling relations of H/N with grafting density were different in these regimes, we plot the dependence of the PAA wet thickness (H) on the solution ionic strength (IS) at pH = 5.8 for various grafting densities in OB and NB regimes, separately. In Figure 10a, we plot H as a function of σ with IS ranging from 1.56×10^{-6} to 0.1, which is in the OB regime. In Figure 10b, the various symbols denote data collected at IS ranging from 0.1 to 0.75, which is in the NB regime. And we will discuss the results of the experimentally measure H for each regime separately as well.

In the SB regime, H increases with increasing σ at high polymer grafting densities ($\sigma > 0.1$ nm^{-2}). This is a typical behavior for the brush conformations. The transition from the brush regime to the mushroom regime occurs at $\sigma \approx 0.08$ nm^{-2}. The slope for the brush regime is found to range from 0.29 to 0.31, in good agreement with the theoretically predicted value of 1/3. With increasing IS, H decreases and the slope in the $H \sim \sigma^n$ dependence increases. The decrease in polymer swelling is largely due to the screening of the electrostatic interactions by the counterions inside the polymer brush. The increase in the slope suggests that the solution ions move more easily inside the grafted polymer at lower grafting density. With increasing σ, the transport of ions inside the densely packed polymers becomes harder. As a consequence, the screening effects weaken.

In the OB regime, previous theoretical work predicted that the wet thickness of polymer brush should decrease with the grafting density as $H \sim \sigma^{-1/3}$ and should increase with increasing IS[6,10] On the basis of theoretical studies, at the transition between

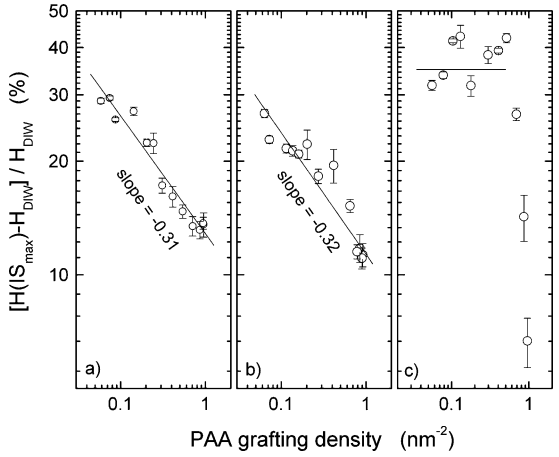

Figure 11. Degree of swelling $[H(\mathrm{IS}_{max}) - H_{DIW}]/H_{DIW}$ for poly(acrylic acid) ($M_n = 4.8$ kDa) as a function of the PAA grafting density in the osmotic brush (OB) regime at pH equal to (a) 4, (b) 5.8, and (c) 10. The points represent average values over three measurements on the sample taken at different positions on the same having the same PAA grafting density. The lines represent the least-squares fits to the data with slopes given in the figure.

the OB to SB regimes (at IS_{max}), H is independent of the brush grafting density. Similar to previous experiments by others,[51] we observe that this scaling relation is somehow flawed. Specifically, by fitting the data in the brush regime to $H \sim N\sigma^n$, we obtain n that ranges from 0.28 to 0.34 instead of the expected value of $-1/3$.

A close inspection of the data in Figure 10a reveals that polymer swelling increases with increasing ionic strength. Interestingly, the value of the exponent n decreases systematically as the solution IS increases. This is in contrast to the performance of PAA in the SB regime, where the value of n increased with increasing IS (cf. Figure 10b). This behavior reveals that when a small amount of salt is added in the OB regime to polymers with a low σ, the grafted polymer swells more relative to PAA at high σ.

In order to quantify this behavior, we define a degree of swelling (DS) of a grafted polymer as

$$\mathrm{DS} = \frac{H(\mathrm{IS}) - H_{\mathrm{DIW}}}{H(\mathrm{DIW})} \times 100\% \qquad (6)$$

where H(IS) and H_{DIW} are the PAA thicknesses evaluated at a given IS and in "pure" water (IS $\rightarrow$ 0), respectively. In Figure 11, we plot the degree of swelling at IS_{max} as a function of the PAA grafting density at different pH values for polymers in the OB regime.

By fitting the data to DS $\sim \sigma^n$, we find n to be very close to $-1/3$ in the OB regime for pH = 4 and 5.8, and 0 for the pH = 10 data. These data reveal that PAA behaves as a weak polyelectrolyte at low pH; here the degree of swelling changes with the σ. And at pH = 10, almost all charges along the polymer backbone are activated and present at the backbone. Recent work showed that the strong polyelectrolyte has independent degree of swelling on the σ.[19] As a consequence, the polymer behavior closely resembles that of a strong polyelectrolyte, whose degree of expansion is independent of the polymer grafting density.

In the following paper,[42] we present our experimental results pertaining to the effect of the PAA molecular weight on PAA brush height. In addition, we use molecular theory of charged polymer brushes to reproduce our experimental findings and provide insight into parameters and structural details that are either hard to measure or are not experimentally accessible.

Conclusions

In order to facilitate the complete exploration of the surface behavior of weak polyelectrolyte (PAA), we created surface-grafted PAA on flat silica-covered substrate with a spatial variation of the chain grafting density. The surface-bound PAA with a gradual variation of grafting densities was formed by the following: (1) creating a molecular density gradient of the surface-anchored polymerization initiator, (2) performing ATRP of poly(*tert*-butyl acrylate) (PtBA) from the surface, and (3) converting the PtBA into PAA by hydrolysis. We used spectroscopic ellipsometry to measure the wet thickness of the PAA as a function of σ, IS, and pH. Here we first reported some experimental observations of the solution behavior of surface grafted poly(acrylic acid) (PAA) as a function of the solution IS and the wet thickness dependence on the grafting density σ.

The wet thickness (H) of the surface-grafted PAA brushes was found to have a nonmonotonic dependence on the ionic strength (IS) of the solution. With increasing concentration of the external salt, the polymer thickness in solution increased and reached a maximum at a certain ionic strength (IS_{max}) and then further decreased. Guided by the theoretical models of weak polyelectrolyte brushes, we have identified three regimes: the osmotic brush (OB), the salted brush (SB), and the neutral brush (NB) regime. By comparing the swelling of polymer under different pH solution conditions, we concluded that the expansion of the grafted chain at low pH value was much less than that at high pH solution.

Accordingly, we studied the H dependence on σ in SB and OB regime. In the SB regime, H was found to increase with increasing σ at high polymer grafting densities, a typical behavior for polymer brushes. The slope for the brush regime ranged from 0.29 to 0.31, in a good agreement with the theoretically predicted 1/3. The transition from the brush to the mushroom regime was found to occur at $\sigma \approx 0.08$ nm^{-2}. In the OB regime, our data revealed that at high σ, H followed the scaling law $H \sim \sigma^n$, with n ranging from 0.28 to 0.34. We commented that this observation was in contrast to the theory, which predicts that in the OB regime $H \sim \sigma^{-1/3}$. We also observed that the degree of polymer swelling increased with increasing IS. The exponent in the $H \sim \sigma^n$ dependence decreased with increasing IS. This behavior was exactly opposite to that detected in the SB regime, where n increased with increasing IS. By defining a degree of swelling (DS) parameter, we fitted the data to DS $\sim \sigma^n$. we found n to be very close to $-1/3$ in the OB regime for pH = 4 and 5.8 and 0 at pH = 10. We rationalized that this behavior was a consequence of the conformational changes in the polymer associated with the concentration of the charges along the backbone.

Acknowledgment. This work is supported by the National Science Foundation. The NEXAFS experiments are carried out at the National Synchrotron Light Source, Brookhaven National Laboratory, which is supported by the U.S. Department of Energy. The authors thank Dr. Kirill Efimenko (NCSU) and Dr. Daniel Fischer (NIST) for their assistance during the course of the NEXAFS experiments. We also thank Professor Saad Khan for allowing us to use his group's FTIR setup. PV thanks the Ministry of Education, Youth, and Sports of the Czech Republic for financial support (Grant 1P05ME753).

Supporting Information Available: Text discussing the conversion of the polymers synthesised on the surface and a figure

showing FTIR spectra from the surfaces covered with PtBA and PAA brushes prepared using the surface-initiated polymerization. This material is available free of charge via the Internet at http://pubs.acs.org.

References and Notes

(1) Fleer, G. J.; Cohen-Stuart, M. A.; Scheutjens, J. M. H. M.; Cosgrove, T.; Vincent, B. *Polymers at Interfaces*; Chapman & Hall: London, 1993.
(2) Halperin, A.; Tirrell, M.; Lodge, T. P. *Adv. Polym. Sci.* **1991**, *100*, 31.
(3) Milner, S. T. *Science* **1991**, *251*, 905.
(4) Szleifer, I.; Carignano, M. A. *Adv. Chem. Phys.* **1996**, *96*, 165.
(5) Pincus, P. *Macromolecules* **1991**, *24*, 2912.
(6) Zhulina, E. B.; Birshtein, T. M.; Borisov. O. V. *Macromolecules* **1995**, *28*, 1491.
(7) Zhulina, E. B.; Borisov, O. V. *J. Chem. Phys.* **1997**, *107*, 5952.
(8) Israëls, R.; Leermakers, F. A. M.; Fleer, G. J.; Zhulina, E. B. *Macromolecules* **1994**, *27*, 3249.
(9) Fleer, G. J. *Ber. Bunsen-Ges. Phys. Chem.* **1996**, *100*, 936.
(10) Israëls, R.; Leermakers, F. A. M.; Fleer, G. J. *Macromolecules* **1994**, *27*, 3087.
(11) Israëls, R.; Leermakers, F. A. M.; Fleer, G. J. *Macromolecules* **1995**, *28*, 1626.
(12) Lyatskaya, Yu. V.; Leemarkers, F. A M.; Fleer, G. J.; Zhulina, E. B.; Birshtein, T. M. *Macromolecules* **1995**, *28*, 3562.
(13) Nap, R.; Gong, P.; Szleifer, I. *J. Polym. Sci. B* **2006**, *44*, 2638.
(14) Kelly, T. W.; Schorr, P. A.; Johnson, K. D.; Tirrell, M.; Frisbie, C. D. *Macromolecules* **1998**, *31*, 4297.
(15) Mir, Y.; Auroy, P.; Auvray, L. *Phys. Rev. Lett.* **1995**, *75*, 2863.
(16) Ahrens, H.; Förster, S.; Helm, C. A. *Phys. Rev. Lett.* **1998**, *81*, 4172.
(17) Guenoun, P.; Muller, F.; et al. *Phys. Rev. Lett.* **1998**, *81*, 3872.
(18) Biesalski, M.; Rühe J. *Macromolecules* **1999**, *32*, 2309.
(19) Biesalski, M.; Rühe J. *Macromolecules* **2002**, *35*, 499.
(20) Biesalski, M.; Rühe, J. *Macromolecule* **2004**, *37*, 2196.
(21) Kurihara, K.; Kunitake, T.; Higashi, N.; Niwa, M. *Langmuir* **1992**, *8*, 2087.
(22) Kim, H. G.; Lee, J. H.; Lee, H. B.; Jhon, M. S. *J. Colloid Interface Sci.* **1993**, *157*, 82.
(23) Currie, E. P. K.; Sieval, A. B.; Fleer, G. J.; Cohen Stuart, M. A. *Langmuir* **1999**, *15*, 7116.
(24) Currie, E. P. K.; Sieval, A. B.; Fleer, G. J.; Cohen Stuart, M. A. *Langmuir* **2000**, *16*, 8324.
(25) Wu, T.; Efimenko, K.; Genzer, J. *J. Am. Chem. Soc.* **2002**, *124*, 9394.
(26) Wu, T.; Efimenko, K.; Vlèek, P.; Šubr, V.; Genzer, J. *Macromolecules* **2003**, *36*, 2448.
(27) Patter, T. E.; Xia, J.; Abernathy, T.; Matyjaszewski, K. *Science* **1996**, *272*, 866.
(28) Coessens, V.; Pintauer, T.; Matyjaszewski, K. *Prog. Polym. Sci.*, **2001**, *26*, 337.
(29) Matyjaszewski, K.; Miller, P. J.; Shukla, N.; Immaraporn, B.; Gelman, A.; Luokala, B. B.; Siclovan, T. M.; Kickelbick, G.; Vallant, T.; Hoffmann, H.; Pakula, T. *Macromolecules* **1999**, *32*, 8716.
(30) Davis, K. A.; Matyjaszewski, K. *Macromolecules* **2000**, *33*, 4039.
(31) Li, D.; Sheng, X.; Zhao, B. *J. Am. Chem. Soc.* **2005**, *127*, 6248.
(32) Park, Y. S.; Ito, Y.; Imanishi, Y. *Chem. Mater.* **1997**, *9*, 2755. Zhang, H. J.; Ito, Y. *Langmuir* **2001**, *17*, 8336. Wang, Y.; Liu, Z. M.; Han, B. X.; Dong, Z. X.; Wang, J. Q.; Sun, D. H.; Huang, Y.; Chen, G. W. *Polymer* **2004**, *45*, 855. Hollman, A. M.; Scherrer, N. T.; Cammers-Goodwin, A.; Bhattacharyya, D. *J. Membr. Sci.* **2004**, *239*, 65.
(33) Liu, G. J. *Macromol. Symp.* **1997**, *113*, 233. Bendejacq, D.; Ponsinet, V.; Joanicot, M. *Eur. Phys. J. E*, **2004**, *13*, 3. Bendejacq, D.; Joanicot, M.; Ponsinet, V. *Eur. Phys. J. E* **2005**, *17*, 83−92.
(34) Abraham, T.; Kumpulainen, A.; Xu, Z.; Rutland, M.; Claesson, P. M.; Masliyah, J. *Langmuir* **2001**, *17*, 8321.
(35) Wittemann, A.; Haupt, B.; Ballauff, M. *Phys. Chem. Chem. Phys.* **2003**, *5*, 1671. Wittemann, A.; Haupt, B.; Merkle, R.; Ballauff, M. *Macromol. Symp.* **2003**, *191*, 81. Rosenfeldt, S.; Wittemann, A.; Ballauff, M.; Breininger, E.; Bolze, J.; Dingenouts, N. *Phys. Rev. E*, **2004**, *70*, 061403. Czeslik, C.; Jackler, G.; Steitz, R.; von Grunberg, H. H. *J. Phys. Chem. B* **2004**, *108*, 13395. Czeslik, C.; Jackler, G.; Hazlett, T.; Gratton, E.; Steitz, R.; Wittemann, A.; Ballauff, M. *Phys. Chem. Chem. Phys.* **2004**, *6*, 5557. Hollmann, O.; Czeslik, C. *Langmuir* **2006**, *22*, 3300. Dai, J. H.; Bao, Z. Y.; Sun, L.; Hong, S. U.; Baker, G. L.; Bruening, M. L. *Langmuir* **2006**, *22*, 4274.
(36) Chen, H.; Hsieh, Y. L. *Biotech. Bioeng.* **2005**, *90*, 405.
(37) Konradi, R.; Rühe, J. *Macromolecules* **2005**, *28*, 4345.
(38) Li, D. J.; Sheng, X.; Zhao, B. *J. Am. Chem. Soc.* **2005**, *127*, 6248. LeMieux, M. C.; Lin, Y. H.; Cuong, P. D.; Ahn, H. S.; Zubarev, E. R.; Tsukruk, V. V. *Adv Funct. Mater.* **2005**, *15*, 1529.
(39) Bell, N. S.; Sindel, J.; Aldinger, F.; Sigmund, W. M. *J. Colloid Interface Sci.* **2002**, *254*, 296. Boyes, S. G.; Akgun, B.; Brittain, W. J.; Foster, M. D. *Macromolecules* **2003**, *36*, 9539. Wang, C. W.; Moffitt, M. G. *Langmuir* **2004**, *20*, 11784. Wang, C.W.; Moffitt, M.G. *Langmuir* **2005**, *21*, 2465. He, L. H.; Zhang, Y. H.; Ren, L. X.; Chen, Y. M.; Wei, H.; Wang, D.J. *Macromol. Chem. Phys.* **2006**, *207*, 684.
(40) Guo, X.; Ballauff, M. *Langmuir* **2000**, *16*, 8719. Dingenouts, N.; Merkle, R.; Guo, X.; Narayanan, T.; Goerigk, G.; Ballauff, M. *J. Appl. Cryst.* **2003**, *36*, 578. Wang, J.; Somasundaran, P. *Colloids Surf. A*, **2006**, *173*, 63.
(41) Wu, T.; Genzer, J.; Gong, P.; Szleifer, I.; Vlèek, P.; Šubr, V. Behavior of surface-anchored poly(acrylic acid) brushes with grafting density gradients on solid substrates. In *Polymer Brushes*; Brittain, B., Advincula, R., Rühe, J., Caster, K., Ed.; Wiley & Sons: New York, 2004.
(42) Gong, P.; Wu, T.; Genzer, J.; Szleifer, I. *Macromolecules*, **2007**, *40*, 8765.
(43) Matyjaszewski, K.; Miller, P. J.; Shukla, N.; Immaraporn, B.; Gelman, A.; Luokala, B. B.; Siclovan, T. M.; Kickelbick, G.; Vallant, T.; Hoffmann, H.; Pakula, T. *Macromolecules* **1999**, *32*, 8716.
(44) Chaudhury, M. K.; Whitesides, G. M. *Science* **1992**, *256*, 1539.
(45) Trial-and-error experiments conducted at different temperatures ranging from −20 to +25 °C revealed that the BMPUS deposited at −10 °C formed best-organized self-assembled monolayers (SAMs) with thickness of 1.9 nm. Experiments using near-edge absorption fine structure (NEXAFS) spectroscopy revealed that the BMPUS molecules in the SAMs were oriented on the surface with their main molecular axis tilted by about 25 degrees with respect to the substrate normal [Tomlinson, M.R.; Genzer, J. *Chem. Commun.* **2003**, 1350].
(46) Mrkvickova, L.; Danhelka. J. *J. Appl. Polym. Sci.* **1990**, *41*, 1929.
(47) Brandrup, J., Immergut, E. H., Grulke, E. A., Eds.; *Polymer handbook*; Wiley: New York, 1999.
(48) It is the value for poly(*n*-butyl acrylate) from ref 47.
(49) Because we work with a large excess of monomer, the concentration of the initiating centers is much smaller relative to that of the free monomer. This set up thus minimizes the likelihood of intermolecular terminations. The situation may be a bit more complex, as revealed by recent computer simulations of controlled-polymerization from surfaces: Genzer, J. *Macromolecules* **2006**, *39*, 7157.
(50) Stöhr, J. *NEXAFS Spectroscopy*; Springer-Verlag: Berlin, 1992.
(51) An, S. W.; Thirtle, P. N.; Thomas, R. K.; Baines, F. L.; Billingham, N. C.; Armes, S. P.; Penfold, J. *Macromolecules* **1999**, *32*, 2731.

MA0710176